USE OF THE AFWA-AWC TESTBED MESOSCALE ENSEMBLE TO DETERMINE SENSITIVITY OF A CONVECTIVE HIGH WIND EVENT SIMULATION TO BOUNDARY LAYER PARAMETERIZATIONS

Rebecca D. Adams-Selin*

Atmospheric and Environmental Research, Inc.,
Lexington, Massachusetts

1. INTRODUCTION

A new Advanced Research Weather Research and Forecasting (WRF-ARW) model ensemble, the Air Force Weather Agency-Aviation Weather Center Testbed Mesoscale Ensemble (AFWA-AWC Testbed) was created as a collaborative effort between AFWA and the AWC. Its purpose is to look at new methods for using an ensemble model and its products to better predict convection and its associated impacts on aviation. One particular area of interest is severe surface winds generated by squall lines, an important aviation hazard.

Current operational model configurations at the Air Force Weather Agency (AFWA) occasionally do not reproduce the severe surface winds associated with a linear convective system (Evan Kuchera, personal communication). While the intensity of the system appears to be represented well, severe wind gusts are not generated at the surface. One possibility for this could be a lack of mixing created by the boundary layer parameterization within the system. The difficulty of fully representing boundary layer processes with a parameterization scheme, particularly convective boundary layer processes, has been highly recognized (Texiera et al. 2008, Shin and Hong 2011).

Additionally, simulated wind and thermodynamic fields above the boundary layer are also affected by these schemes. For example, Carter et al. (2011) examined model reproductions of low-level jets as compared to observations using a variety of boundary layer parameterizations. They found the Mellor-Yamada-Janjic (MYJ; Janjic 1994) and Quasi-Normal Scale Elimination (QNSE; Sukoriansky et al. 2005) boundary layer parameterizations best represented the speed of the low-level jet, but consistently under-predicted the height. Meanwhile, the Yonsei University (YSU; Hong et al. 2006) and Mellor-Yamada-Nakanishi-Niino 3.0 (MYNN3; Nakanishi and Niino 2004, 2006) simulations under-represented the jet speed, and generally over-predicted the height. While the reasons for such discrepancies are unclear, it is evident that these parameterization schemes affect more of the model simulation than "just" the boundary layer.

The AFWA-AWC Testbed is used to analyze sensitivity of a squall line high-wind event simulation to differing boundary layer parameterization schemes. The goals of this experiment are two-fold: first, to examine what differences in a set of simulations are produced by variation in the boundary layer parameterization. This will help determine the amount of "spread", or differences between ensemble members, that can be expected from these variations. Secondly, the ability of each simulation to generate strong surface winds in a convective system will be studied.

2. EXPERIMENT DESCRIPTION

The AFWA-AWC Testbed Mesoscale Ensemble contains ten members, designed by AFWA to cover the largest spread of convective possibilities given the current parameterizations. It utilizes WRF-ARW version 3.2.1. There are four different sets of initial conditions, eight different microphysics schemes, three concentration levels of initial cloud condensation nuclei (CCN), and four unique boundary layer parameterizations. However, for this study, only one microphysics parameterization, set of initial conditions, and initial CCN concentration was used, to better isolate the effects of the boundary layer parameterization. The Navy's Operational Global Atmospheric Prediction System (NOGAPS) model was used to provide initial conditions at one-degree horizontal resolution and six-hour temporal resolution. The WRF Double-Moment 5-class microphysics scheme was selected, and its default initial CCN concentration of 1E8 m^{-3} was used.

**Corresponding author address:* Rebecca Adams-Selin, 16th Weather Squadron, HQ AFWA, 101 Nelson Dr. Offutt AFB, NE 68113; rebecca.selin.ctr@offutt.af.mil

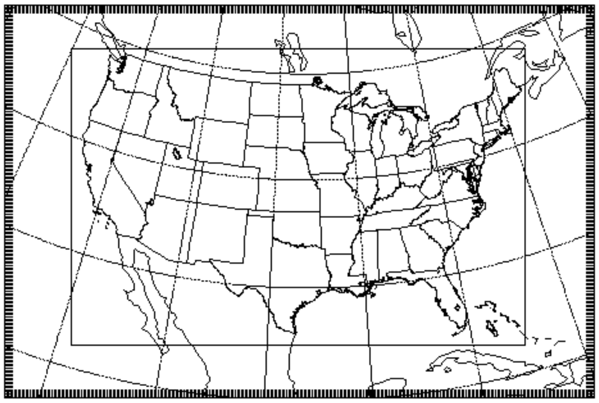

Figure 1: AFWA-AWC Testbed Mesoscale Ensemble domain. Later figures will show only a subsection of the domain over the southeast U. S. for space considerations.

The model was initialized at 0000 UTC on 4 April 2011 and run for 24 hours. The rest of the model configuration, including the domain sizes and locations, are those used for the AFWA-AWC Testbed MesoscaleEnsemble. The parent domain has 20 km horizontal resolution; the nested domain 4 km resolution. Both are shown in Fig. 1. Thirty-five vertical levels are used, with a higher concentration of levels in the boundary layer. Other parameterizations include the Noah land surface model, the Rapid Radiative Transfer Model longwave radiation scheme, and the Goddard shortwave radiation scheme. The Kain-Fritsch convective parameterization was used on the parent domain, with explicit convection in the nest; feedback was allowed from the nest to the parent domain. Sensitivity tests were conducted using the four boundary layer parameterizations used in the AFWA-AWC Testbed: YSU, MYJ, QNSE, and MYNN3.

The 4 April 2011 convective high wind event was chosen for simulation. This event was strongly synoptically forced (see next section for description); all ensemble members successfully simulated a strong squall line. Choosing an event of this nature allowed the study to focus on the differences produced by boundary layer schemes within a generated convective system, as opposed to a focus on why one simulation produced the convection and another did not. Additionally, the AFWA operational model configuration, which uses the YSU boundary layer scheme, did not fully simulate these severe surface winds although it did simulation the convection.

3. SYNOPTIC DESCRIPTION

A large squall line mesoscale convective system formed on 4 April 2011 and traveled over 1000 miles across the southeastern United States. It produced an extraordinarily large number of severe wind reports - over 1300 in all. These reports stretched from east Texas and north-central Arkansas through eastern Florida north through North Carolina. Convection first initialized at 1000 UTC over northwest

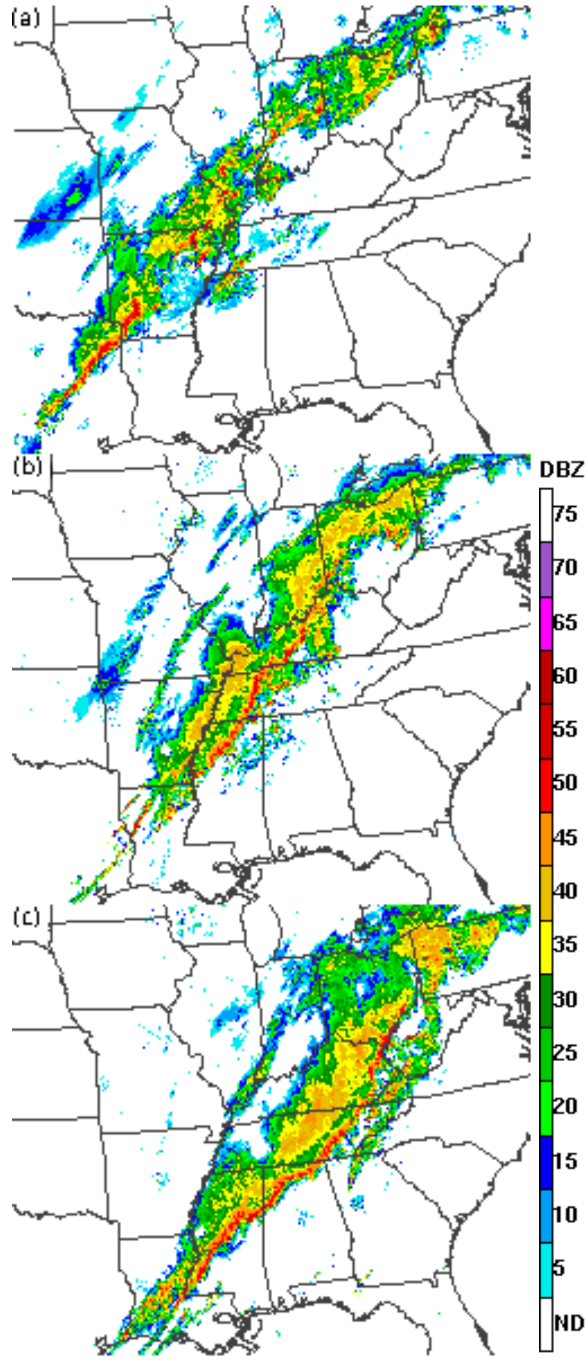

Figure 2: 1400 UTC (a), 1800 UTC (b), 2200 UTC (c) 4 April 2011 base reflectivity mosaic, retrieved from the Storm Prediction Center's Severe Thunderstorm Events database (www.spc.noaa.gov/exper/archive/events).

Arkansas and north-central Texas, and slowly propagated to the east. The convection quickly grew into two convective lines, aligned southwest-to-northeast, with additional cellular convection approximately 100 km ahead at 1230 UTC. By 1400 UTC, bowing segments began to appear along one of the convective lines (Fig. 2a); by 1600 UTC a large bow echo covered all of Arkansas; by 1800 UTC the convective system stretched from central Mississippi to northern Kentucky, with a moderate amount of stratiform precipitation both trailing and parallel to it (Fig. 2b). The system reached its maximum extent in length at 2200 UTC, reaching from central Louisiana to extreme southern Ohio with multiple bowing segments along its length (Fig. 2c). The system continued its eastward trek across the southeast U. S. until reaching the Atlantic coast at 1200 UTC on 5 April.

The 1200 UTC 4 April upper-air analysis (not shown) revealed a strong trough at 250 hPa centered over the western Great Plains. A 60 m s^{-1} jet streak was located on the eastern side of this trough, with the right entrance region over northeast Texas and western Arkansas. Strong upper-level divergence was located over much of the lower Mississippi valley region. At both 700 and 850 hPa, a ridge of increased moisture was located ahead of a strong cold front that stretched from north-central Texas up to southern Michigan. Significant moisture pooling occurred at 850 hPa near the convective initiation point. There was also strong (greater than 30 m s^{-1}) 850 hPa southwesterly flow along this cold front, which would function as inflow into the southern end of the storm (as seen in the 1200 UTC sounding at Jackson, Mississippi, Fig. 3). Strong northwesterly winds (on the order of 20 m s^{-1}) were located behind the cold front. Southwest surface flow was also very strong ahead of the cold front, with gusts above 15 m s^{-1} (Fig. 4). Dewpoints at the convective initiation point were between 13 and 17 ^{o}C; these decreased farther across the southeast U.S. The squall line would form along the surface cold front and propagate eastward with it.

The strong southwest winds from 850hPa down to the surface which provided inflow into the southern end of the system were still evident in the 0000 UTC 5 April 2011 analysis (not shown). South southwest 850 hPa winds of 23 m s^{-1} were reported at Montgomery, Alabama, immediately ahead of the squall line. Increased moisture was still being advected northward by this flow, continuing to provide additional energy to the squall line system.

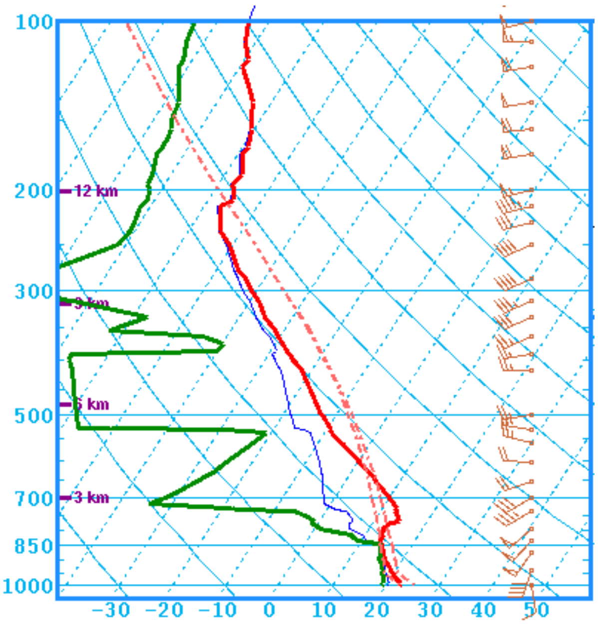

Figure 3: 1200 UTC 4 April 2011 sounding from Jackson, Mississippi (KJAN). Retrieved from the Storm Prediction Center's Severe Thunderstorm Events database (www.spc.noaa.gov/exper/archive/events).

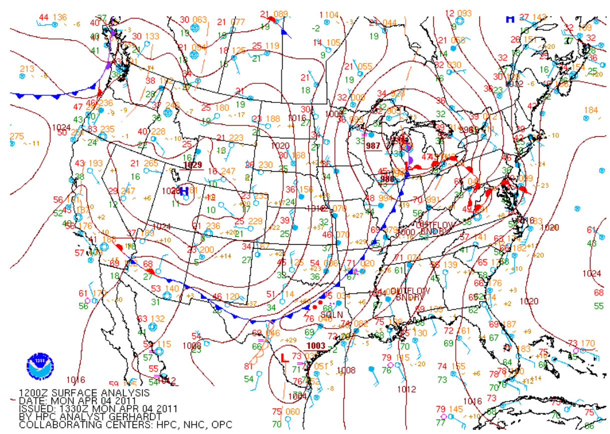

Figure 4: Hydrometeorological Prediction Center surface analysis for 1200 UTC 4 April 2011. Retrieved from the Storm Prediction Center's Severe Thunderstorm Events database (www.spc.noaa.gov/exper/archive/events).

4. RESULTS

4.1 *Storm structure*

Convection in all four simulations initializes in extreme east Kansas at 0200 UTC on 4 April. This convection propagates southeastward until two convective lines form at 1100 UTC. While initial convective development was somewhat different than observed, at this time the simulations generally match the observed radar. One line stretches from southeast Oklahoma to northwest Arkansas, and another

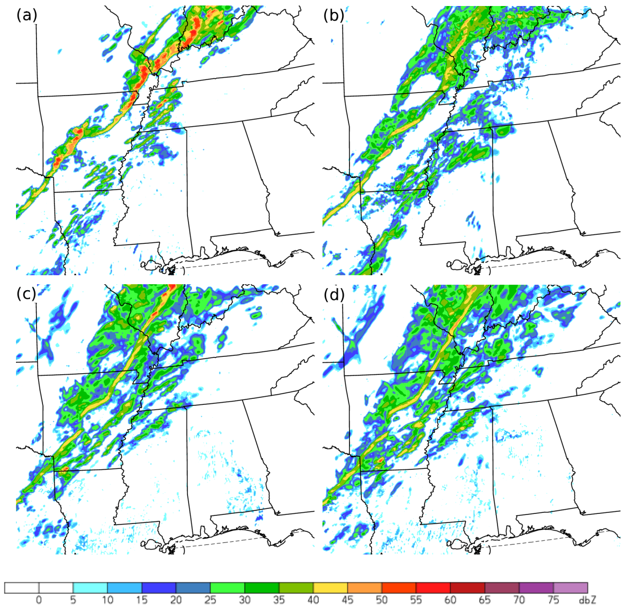

Figure 5: Simulated composite radar reflectivity, as calculated by WRFPOST, at 1400 UTC 4 April 2011. Simulation used the: (a) YSU, (b) MYNN, (c) MYJ, and (d) QNSE boundary layer parameterization.

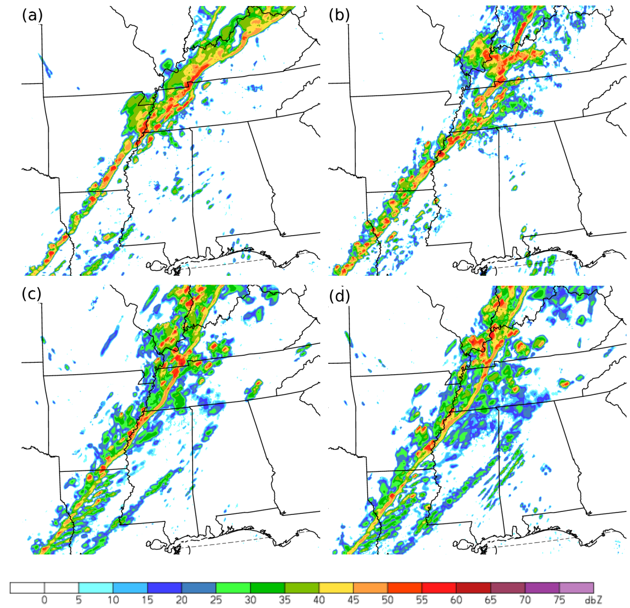

Figure 6: Same as in Fig. 5, but for 1800 UTC.

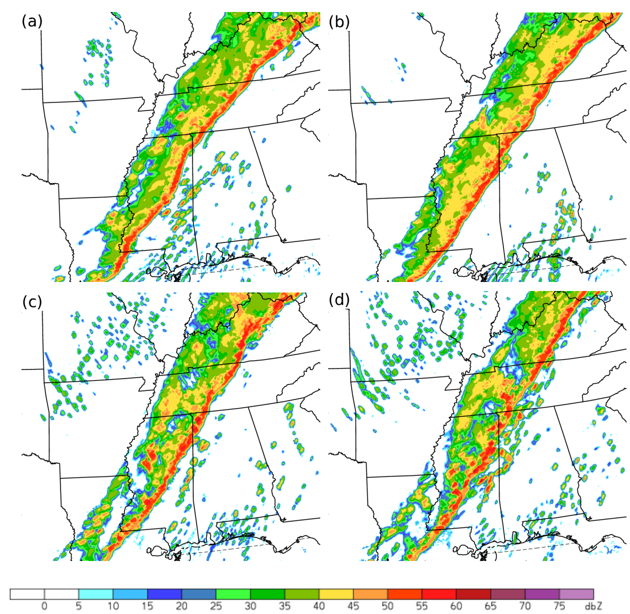

Figure 7: Same as in Fig. 5, but for 2200 UTC.

from north-central Arkansas to southwest Missouri. However, by 1400 UTC, when the observed system is developing bowing segments along the convective line, only the YSU simulation has done the same (Fig. 5a). The other three simulations have barely developed a linear structure, and at this point the convection within is very weak (Figs. 5b,c,d). However, all three of these schemes correctly depict low-intensity stratiform precipitation both in advance of and behind the convective line. The YSU simulation better depicts the convective intensity within the squall line, but not the surrounding stratiform precipitation.

At 1800 UTC, a continuous convective line with embedded bowing segments develops in the MYJ and QNSE simulations (Fig. 6c, d). These simulations correctly depict the Mississippi-Tennessee portion of the line, but incorrectly extend the line southward through Louisiana. The YSU simulation still better displays the convective intensity, but at this point contains no bowing segments and still minimal stratiform precipitation (Fig. 6a). This simulation also stretches too far south through Louisiana. The MYNN3 simulation is still struggling with developing a linear convective system, instead developing a number of intense convective cells over instead (Fig. 6b).

Finally, all simulations develop a strong, continuous convective line by 2200 UTC. The convective lines in the YSU and MYNN3 simulations are very linear, uniform, and unbroken (Figs. 7a,b); the MYJ has slightly more cellular development within the system (Fig. 7c); the QNSE is very cellular particularly at the southern end of the convection (Fig. 7d). The placement of the southern end of the convection is approximately the same in all of the simulations. The faster movement of the northern end of the convective line is better captured by the MYNN3 and YSU simulations. Both of the YSU and MYJ simulations have developed bowing segments repeatedly over the last four hours, although all four simulations exhibit some bowing at this point. Addition-

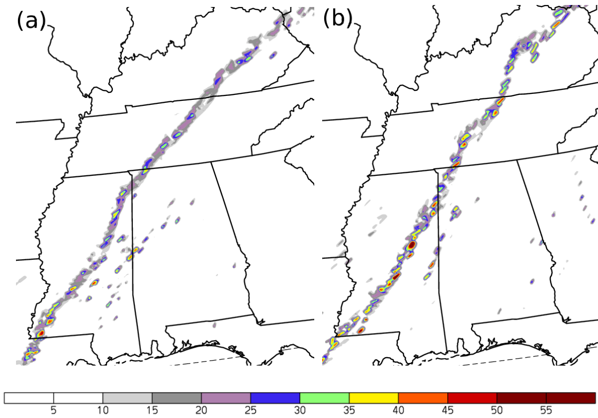

Figure 8: Maximum updraft velocity (m s^{-1}) at 2200 UTC 4 April for the (a) YSU and (b) MYJ simulations. These simulations were the two extremes of system intensity; the MYNN and QNSE simulations' maximum updraft speeds fell in between, as discussed. The AFWA-developed maximum updraft velocity diagnostic variable is shown.

ally, all of the simulations contain some amount of stratiform rain, although none as much as observed. The simulations also all develop some isolated cellular convection ahead of and behind the main system, with the QNSE and MYJ forming the most, and the MYNN3 the least.

As all four simulations appear to produce approximately equal maximum composite reflectivity by 2200 UTC, maximum updraft speed at that time was examined to more directly determine the strength of the storm. The MYJ simulation system has the most numerous, and fastest, updraft cores along the length of the convective line (Fig. 8b). The QNSE simulation has similar updraft speeds, but fewer overall cores. The system in the MYNN3 simulation has approximately the same number of updraft cores, but with slower peak speeds. Finally, the YSU system updrafts were much slower and much less numerous (Fig. 8a). Peak updraft speeds were approximately 10 m s^{-1} faster in the MYJ system versus the YSU system. Downdraft speeds appeared approximately equal, between 5 and 10 m s^{-1} all along each convective line, with a few pockets of 15 m s^{-1}.

4.2 *Boundary layer development*

Model soundings from Jackson, Mississippi are chosen to examine the development of the environmental boundary layer ahead of the system. In all of the simulations, the lower levels begin immediately after initialization as a the sun sets. The QNSE boundary layer stabilizes entirely first, at 0400 UTC; the MYJ boundary layer follows at 0500 UTC. The MYNN3 and YSU boundary layers never entirely stabilize; the YSU simulation has a well-mixed dry adiabatic layer extend from 900 hPa to the surface even at 0500 UTC. Above this, an inversion is present in all of the simulations at 0500 UTC, reaching approximately 15^{o}C at 800 hPa.

At 1000 UTC (500 AM LDT) the surface layer in all simulations begins warming with the sunrise. All of the simulations contain a layer at or near saturation; in the MYJ, QNSE, and MYNN simulations this layer is thicker (in the MYJ case, almost 50 hPa deep) and much closer to the surface with only a very thin mixed layer above the surface (Figs. 9b,c,d). The YSU simulations has a much deeper, drier, mixed layer (100 hPa deep) with a thin, near-saturation layer above (Fig. 9a). All the simulations contain a large capping inversion, but the peak of the inversion in the MYJ and QNSE is lower than in the other two. Compared to the observed 1200 UTC KJAN sounding (Fig. 3), all of the inversions are too strong and extend over too deep a layer.

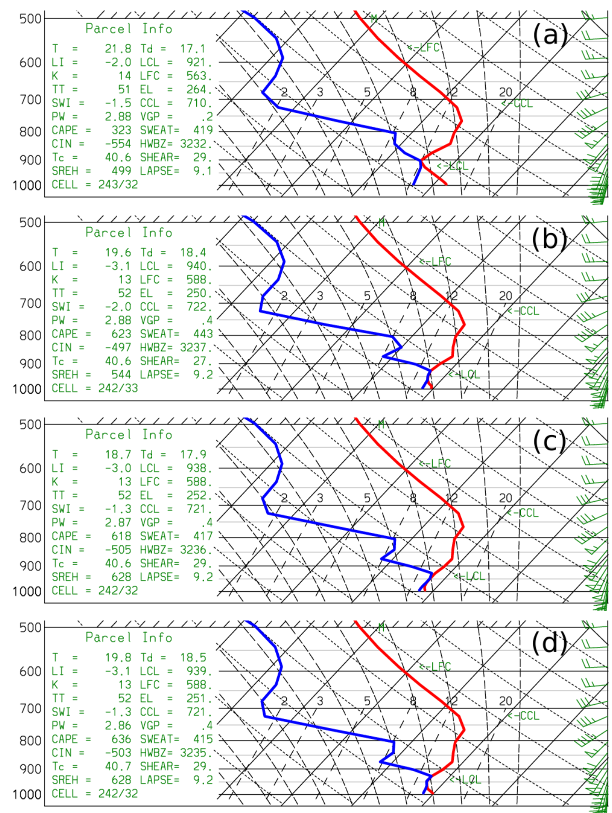

Figure 9: Model soundings from station KJAN (Jackson, MS) at 1000 UTC 4 April 2011. Simulation used the: (a) YSU, (b) MYNN, (c) MYJ, and (d) QNSE boundary layer parameterization.

By 1600 UTC, the 850 hPa cold front had ar-

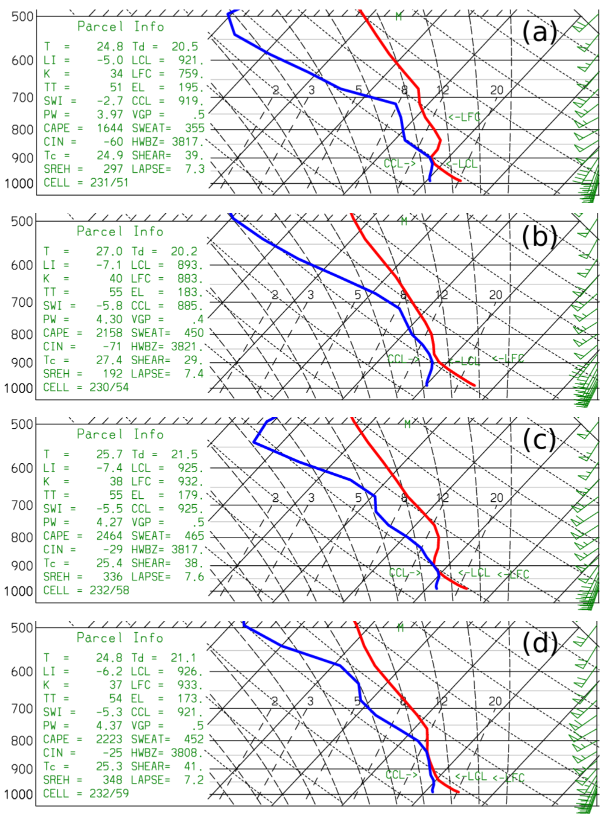

Figure 10: As in Fig. 8, but for 2000 UTC.

rived, bringing with it cooler air aloft and eroding the capping inversion in the MYJ, MYNN3, and QNSE simulations. The mid-levels had cooled in the YSU system, but an inversion still remains, with 118 J kg^{-1} of convective inhibition (CIN) and a level of free convection (LFC) of 609 hPa. The CINs and LFCs of the other three simulations are between 10 and 16 J kg^{-1}, and 938 hPa, respectively.

These differences continue through 2000 UTC, immediately prior to the arrival of the squall line at KJAN (Figs. 10a-d). At this point, the MYJ and QNSE simulation soundings showed more moisture in the lower levels near the surface compared to the MYNN3 and YSU soundings, as well as significantly lower LFCs (932 hPa in the MYJ versus 759 hPa in the YSU), and significantly higher CAPEs (on the order of 300 to 800 J kg^{-1} higher). Thus, it is to be expected that the system formed in the MYJ simulation would be strongest, if looking solely at instability availability. The QNSE would be expected to be slightly weaker, and the MYNN3 and YSU systems the weakest. These predictions match well with the system strengths inferred from the maximum updraft speeds in Section 4.1.

However, the YSU and MYNN3 soundings at this time also have well-mixed dry adiabatic layers extending from approximately 900 hPa to the surface (Figs. 10a,b), generated by strong mixing within the boundary layer schemes. This mixing would more easily carry the horizontal momentum generated aloft by the convective system to the surface. The QNSE sounding has only a very minimal mixed layer. Thus, while the YSU and MYNN3 systems might be weaker, whatever horizontal momentum each system did generate would be easily translated to the surface. This translation would be most difficult in the QNSE system.

4.3 *Horizontal wind speed*

At 1800 UTC the QNSE and MYJ simulations were producing 25 m s^{-1} surface wind gusts over large areas of the domain in eastern Kentucky and Tennessee, far ahead of the convective system. These incredibly strong surface winds are unrealistic: observed gusts at that time ranged were 15 to 20 m s^{-1}. These strong winds are not produced by the YSU and MYNN3 simulations. However, the lesser intensity of the wind gusts generated along the convective line in the YSU and MYNN3 simulations (approximately 15 to 20 m s^{-1}) is unrealistic as well, as severe wind reports (greater than 25 m s^{-1}) were being generated along the entire length of the squall line. Only the MYJ simulation produces severe winds the entire length of the squall line at this time.

Moving to time of full maturity of the system, at 2200 UTC, only the MYJ and QNSE reproduce the intensity of the severe winds the length of the convective system (Figs. 11c,d). However, these same simulations also act to overproduce the strength of the wind gusts ahead of the convection in eastern Tennessee and Kentucky by approximately 10 m s^{-1}. The YSU and MYNN3 simulations do a better job recreating the surface wind gusts ahead of the storm, but only produce a few isolated spots of severe wind along the length of the convective line (Figs .11a,b).

Winds at 850 hPa provide another clue for the differing surface wind speeds. Examination of the observed 850hPa wind field at 1200 UTC on 4 April (not shown) shows speeds of 30 m s^{-1} common from central Arkansas northeast through Ohio, ahead of and along the cold front. The MYJ and QNSE simulations faithfully reproduce these speeds, but the YSU most definitely does not, with wind speeds reaching only 25 to 30 m s^{-1}. Slower inflow into the system would also result in a less intense system, and therefore less intense surface winds.

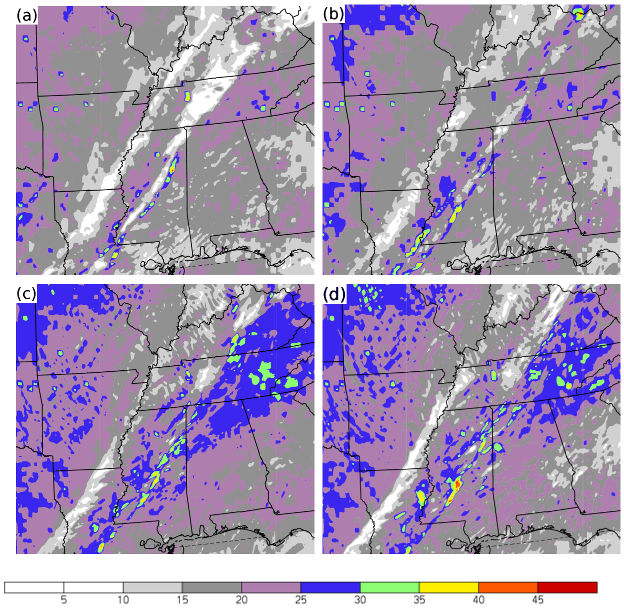

Figure 11: Simulated maximum 10-m wind gusts (m s^{-1}) at 2200 UTC 4 April 2011 for the (a) YSU, (b) MYNN, (c) MYJ, (d) QNSE boundary layer parameterization. The AFWA-developed 10-m wind gust diagnostic variable is shown.

5. CONCLUSIONS

Changes in boundary layer parameterizations can create a wide variety of responses in a convective simulation. Specifically, rates of boundary layer stabilization and destabilization are affected by these changes, and through them the convective intensity, amount of stratiform precipitation, strength of system, and low-level and surface wind speed are also varied. The YSU and MYNN3 boundary layer schemes appeared more aggressive with mixing, resulting in deeper, drier mixed layers near the surface. The MYJ and QNSE schemes appeared to simulate less mixing, particularly at night, allowing the boundary layer to moisten. After the convection developed, the YSU simulation was the first to capture the full intensity of the system, but it was unable to sustain that intensity, and only slowly developed the associated stratiform precipitation. The MYJ simulation, while slower to develop the convective intensity, was able to sustain it.

Results here also showed that in this set of simulations the largest contribution to changes in convective surface winds was the effected change in storm intensity. More boundary layer mixing, such as found in the YSU and MYNN3 schemes, would be expected to better translate horizontal momentum aloft to the surface. Here this mixing was actually a detractor, acting to dry out the boundary layer in advance of the simulated system. This resulted in a less intense system and therefore less intense surface winds. The MYJ and QNSE simulations created stronger surface winds by first simulating stronger convective systems.

Future work will include idealized simulations of these factors, allowing generalization of these concepts independently of synoptic effects. Simulation of a less synoptically forced system, such as air-mass thunderstorms, would also aid in this endeavor.

6. ACKNOWLEDGEMENTS

Computing resources were provided by the Navy Department of Defense Supercomputing Resource Center (Navy DSRC) and the Army Research Laboratory Department of Defense Supercomputing Resource Center (ARL DSRC), which are sponsored by the DoD High Performance Computing Modernization Program. This research was conducted under the Cooperative Research Data Agreement between the Air Force Weather Agency and Atmospheric Environmental Research, Inc.

7. REFERENCES

Carter, K. C. A. J. Deppe, and W. A. Gallus, Jr. 2011: Simulations of nocturnal LLJs with a WRF PBL scheme ensemble and comparison to observations from the ARM project. *20th Conf. on Numerical Weather Prediction*, Seattle, WA, Amer. Meteor. Soc. P474.

Hong, S.Y. and Y. Noh, 2006: A new vertical diffusion package with an explicit treatment of entrainment processes. *Mon. Wea. Rev.*, **134**, 2318–2341.

Janjic, Z. I. 1994: The stop-mountain eta coordinate model: Further developments of the convection, viscous sublayer, and turbulence closure schemes. *Mon. Wea. Rev.*, **122**, 927–945.

Nakanishi, M. and H. Niino, 2006: An improved Mellor-Yamada level-3 model: Its numerical stability and application to a regional prediction of advection fog. *Bound.Layer Meteor.*, **119**, 397–407.

——, and H. Niino, 2004: An improved Mellor-Yamada level-3 model with condensation physics: Its design and verification. *Bound.Layer Meteor.*, **112**, 1–31.

Shin, H.H. and S.Y. Hong, 2011: Intercomparison of planetary boundary-layer parametrizations in the WRF model for a single day from CASES-99. *Bound.Layer Meteor.*, **139**, 261–281.

Sukoriansky, S. B. Galperin, and V. Perov, 2005: Application of a new spectral theory of stably stratified turbulence ot the atmospheric boundary layer over sea ice. *Bound.Layer Meteor.*, **117**, 231–257.

Teixeira, J. B. Stevens, C. S. Bretherton, R. Cederwall, J. D. Doyle, J. C. Golaz, A. A. M. Holtslag, S. A. Klein, J. K. Lundquist, D. A. Randall, A. P. Siebesma, and P. M. M. Soares, 2008: Parameterization of the atmospheric boundary layer: A view from just above the inversion. *Bull. Amer. Meteor. Soc.*, **89**, 453–458.